CSIRO PUBLISHING

Aust. J. Chem.
http://dx.doi.org/10.1071/CH12484

Full Paper

Ni/MWCNT-Supported Palladium Nanoparticles as Magnetic Catalysts for Selective Oxidation of Benzyl Alcohol

Mingmei Zhang,[A] *Qian Sun,*[A] *Zaoxue Yan,*[A] *Junjie Jing,*[A] *Wei Wei,*[A] *Deli Jiang,*[A] *Jimin Xie,*[A,B] *and Min Chen*[A]

[A]School of Chemistry and Chemical Engineering, Jiangsu University, Zhenjiang 212013, China.
[B]Corresponding author. Email: Xiejm391@sohu.com

Well dispersed Pd@Ni bimetallic nanoparticles on multi-walled carbon nanotubes (Pd@Ni/MWCNT) are prepared and used as catalysts for the oxidation of benzyl alcohol. Scanning electron microscopy, transmission electron microscopy, energy-dispersive X-ray spectroscopy analysis, and X-ray diffraction were performed to characterise the synthesised catalyst. The results show a uniform dispersion of Pd@Ni nanoparticles on MWCNT with an average particle size of 4.0 nm. The as synthesised catalyst was applied to the oxidation of benzyl alcohol. A 99 % conversion of benzyl alcohol and a 98 % selectivity of benzaldehyde were achieved by using the Pd@Ni/MWCNT (Pd: 0.2 mmol) catalyst with water as a solvent and H_2O_2 as oxidant at 80°C. The catalytic activity of Pd@Ni/MWCNT towards benzyl alcohol is higher than that of a Pd/MWCNT catalyst at the same Pd loadings. The catalyst can be easily separated due to its magnetic properties.

Manuscript received: 23 October 2012.
Manuscript accepted: 11 January 2013.
Published online: 20 February 2013.

Introduction

Selective oxidation of benzyl alcohol on noble-metal-based catalysts has been widely studied during the past decades.[1–6] Other than hydrogen peroxides, gas phase oxidation at an elevated temperature by air/O_2 also provides an alternative route.[3,4] Palladium (Pd) as a most versatile catalyst ingredient has been widely used in organic reactions.[5,6] As a promising way to achieve larger catalyst utilisation, supports were adopted to disperse the Pd nanoparticles with a smaller size, which greatly improved the ratio of use of noble metal to catalytic activity. Carbon materials with various shapes as Pd catalyst supports have been intensively investigated due to their low weight, high specific area, and chemical inertia. Yan et al. synthesised three kinds of hollow carbon hemispheres, and loaded Pd nanoparticles using an intermittent microwave heating method, to generate electrocatalysts for alcohol electrooxidation in fuel cells. They found a higher catalytic activity than using the Vulcan XC-72 carbon powder as support.[7,8] Carbon nanotubes (CNT), as novel carbon materials with excellent chemical inertia, are promising supports for catalysts. Xiang et al. has reported that CNT-supported Pd catalysts (Pd/CNT) are more selective for the hydrogenation of acetophenone to give α-phenylethanol than the commercially available, activated carbon-supported Pd catalyst.[9]

Another effective method to enhance the activity of catalysts is to mix other elements with the precious metal to generate intermetallic compounds and alloys, which has been proven to be an effective method in making better use of the precious metal.[10–17] Deplanche et al. synthesised bimetallic Au/Pd nanoparticles supported on bacterial cells and the catalyst showed excellent selectivity towards benzaldehyde in selective oxidations of benzyl alcohol in the absence of solvent and without a base.[10] Pd as one of noble metals occurs in nature at very low levels of abundance although as a catalysts in various reactions it is highly effective. Hybrid alloy structures of Pd (a noble metal) and Ni (a non-noble metal) not only combines the properties of the individual constituents but also shows an enhancement in specific properties because of the synergistic effects and the rich diversity of the compositions.[18–28] Adzic et al. demonstrated the high activity and long-term stability of a Pt monolayer deposited on a metal, a metal alloy, or core–shell nanoparticles whose activity can surpass that of the state-of-the-art carbon-supported all-Pt electrocatalysts.[24]

In this paper, multiwalled carbon nanotube (MWCNT)-supported Pd@Ni bimetallic nanocatalysts were synthesised by two-steps and their catalytic efficiency for the selective oxidation of benzyl alcohol were studied. The mechanisms toward Pd@Ni/MWCNT, i.e. the formation of Ni-nanoparticle-loaded MWCNT and Pd-salt-loaded Ni/MWCNT, were investigated. The hydrogen peroxide oxidation of benzyl alcohol catalyzed by Pd@Ni/MWCNT nanoparticles was conducted in water for environmental compatibility. The interactions between Ni nanoparticles and Pd nanoparticles, such as crystalline nickel entering into the palladium crystal lattice leading to a synergistic effect, a d-band centre shift,[27] and a Pd skin effect, are favourable for the promotion of the catalytic activity and stability of Pd@Ni/MWCNT. Several experimental parameters, such as amount of catalyst, temperature, reaction time, and the catalytic activity of recycling were systematically studied to evaluate the catalytic performances of Pd@Ni/MWCNT

nanoparticles in the selective oxidation of benzyl alcohol. Pd@Ni/MWCNT exhibited a much higher catalytic activity compared with an equal amount of palladium nanoparticles in the selective oxidation of benzyl alcohol.

Experimental

Preparation of Acid-Treated MWCNT

MWCNT used in this work were purchased from Shenzhen Nanotechnologies Port Co. Ltd (Shenzhen, China) with a diameter of 20–40 nm, length of 6–15 mm, and purity of 98 wt.-%. The MWCNT were purified by refluxing in concentrated nitric acid at 100°C for 12 h, and then washed and filtered with deionised water.[29,30] In order to generate significant amounts of functional groups on the surface of the MWCNT, a typical treatment was as follows:[31] 50 g of MWCNT, 60 mL of H_2SO_4, and 20 mL of HNO_3 were mixed with sonication for 10 min, and then placed in an oil bath at 80°C with vigorous stirring for 1 h. The resulting product was filtered off and washed with deionised water five times, and dried in a vacuum oven at 60°C for 12 h.

Preparation of the Ni/MWCNT Catalyst

To synthesise the Ni/MWCNT compounds, 4 g of acid-treated MWCNT was dispersed in 100 mL of ethylene glycol (EG) by sonication for 60 min. In this reaction, EG acts as a reducing, stabilising, and dispersing agent. Nickel acetate (5 g) was then added to the solution under vigorous stirring, and then subjected to microwave heating in a microwave oven at a temperature of 180°C operated at 750 W. The pH of the entire solution was adjusted to 10 by adding NaOH (2.0 M). At the end of the heating, the solution was cooled to room temperature, and the product was isolated by several washes with distilled water to remove the excess EG and subsequent separation by sintered discs. Finally, the nickel-impregnated MWCNT (Ni/MWCNT) were obtained. The Ni contents were analysed by inductively coupled plasma spectroscopy (ICP, Optima2000DV, USA) analysis, which showed 30.2 wt-% of Ni in the Ni/MWCNT compound.

Preparation of the Pd@Ni/MWCNT Catalyst

Pd@Ni/MWCNT catalysts were synthesised by a replacement method. Typically, 20 mL of 0.372 M H_2PdCl_4 and 2 g of Ni/MWCNT were dispersed in 100 mL of distilled water. The resulting solution was uniformly dispersed by sonification for 10 min, and then vigorously stirred for 14 h at room temperature. The black solid was separated using sintered discs, washed with deionised water five times, and finally dried in a vacuum oven at 60°C. For comparison, Pd nanoparticles supported on MWCNT (Pd/MWCNT) were also obtained directly by reducing H_2PdCl_4 in a MWCNT suspension using formic acid as the reducing agent. The theoretical Pd contents in both Pd@Ni/MWCNT and Pd/MWCNT were targeted at 20 wt-%. ICP analysis gave the actual Pd contents as 19.5 wt-% for Pd@Ni/MWCNT and 19.2 wt-% for Pd/MWCNT.

Procedure for Alcohol Catalytic Oxidation

A conical flask was filled with benzyl alcohol (1.0 mmol), K_2CO_3 (3.0 mmol), Pd@Ni/MWCNT, or Pd/MWCNT (Pd: 0.2 mmol), and H_2O (20.0 mL). The mixture was stirred and dispersed for 1 h before adding freshly prepared H_2O_2 at a given temperature. Upon completion of the reaction the organic products were extracted from the reaction mixture with dichloromethane (20 mL). The extracted organic layer was evaporated on a rotary evaporator, and then analysed by gas chromatography. The recycled organic layer was analysed by a 7890A gas chromatograph (Agilent Technology Inc., San Jose, CA, USA) equipped with a flame-ionisation detector. The GC yield was obtained from the normalisation method.

Measurements

The morphology of the as-prepared samples were examined by scanning electron microscopy (SEM) using a field emission instrument (Hitachi S-4800 II, Japan) and transmission electron microscopy (TEM) (JEOL-JEM-2010, Japan) operating at 120 kV. The phase purity and crystal structure of the obtained samples were examined by X-ray diffraction (XRD) using a D8 Advance X-ray diffractor (Bruker AXS Company, Germany) equipped with $Cu_{K\alpha}$ radiation (λ 1.5406 Å), employing a scanning rate of 0.02 deg s^{-1} in the 2θ range from 10° to 80°. The metal contents of the catalysts were analysed by inductively coupled plasma spectroscopy (ICP, Optima2000DV, USA). The recycled organic layers were analysed by a 7890A gas chromatograph (Agilent Technology Inc., USA) equipped with a flame-ionisation detector and HP-5 capillary column (30 m × 0.32 mm × 0.25 mm), N_2 was the carrier gas, and the following settings were used: column temperature: 120°C, oven temperature: 230°C, temperature of boil room: 250°C. The flow rate of hydrogen, air, and nitrogen were 40, 300, and 30 mL min^{-1}.

Results and Discussion

The Formation Mechanism of Pd@Ni/MWCNT

The schematic illustration for the formation of Pd@Ni/MWCNT nanocomposites is shown in Fig. 1. Once MWCNT was functionalised, it was dispersed thoroughly in EG by sonication for 10 min. Nickel acetate was then added to the solution under vigorously stirring, and the mixture was subjected to microwave heating in a microwave oven. Finally the compound was isolated by several washes with distilled water and monocrystalline nickel nanoparticles supported on MWCNT (Ni/MWCNT) were obtained. After the Ni/MWCNT was added to a H_2PdCl_4 solution and continuously stirred for 14 h, well dispersed Pd@Ni nanoparticles on MWCNT were obtained.

FTIR Spectra Analysis

In order to identify the chemical groups on the surface of the MWCNT, we conducted FTIR experiments and the results are shown in Fig. 2. The broad intense band around 3440 cm^{-1} in Fig. 2a can be attributed to the stretching vibrational mode of O–H groups. This band might have resulted due to –OH functional groups forming during the purification process. The peak at 1638 cm^{-1} is assigned to the C=C stretching of the MWCNT. A small peak at around 1385 cm^{-1} is due to O–H bending deformation in –COOH. For the HNO_3-acid treated MWCNT sample (HNO_3-f-MWCNT, Fig. 2b), the peaks are obviously weak compared to the H_2SO_4/HNO_3-treated MWCNT (H_2SO_4/HNO_3-f-MWCNT, Fig. 2a). Almost no peak can be seen in the non-acid-treated MWCNT (Fig. 2c), which is further evidence that functional groups are generated on the surface of MWCNT by H_2SO_4/HNO_3 acid treatment.

Morphology and Element Analysis

The morphology and particle size of acid-treated MWCNT, Ni/MWCNT, Pd@Ni/MWCNT, and Pd/MWCNT were examined by FESEM and TEM as shown in Fig. 3. Fig. 3a shows a typical SEM image of acid-treated MWCNT. From Fig. 3b and 3d

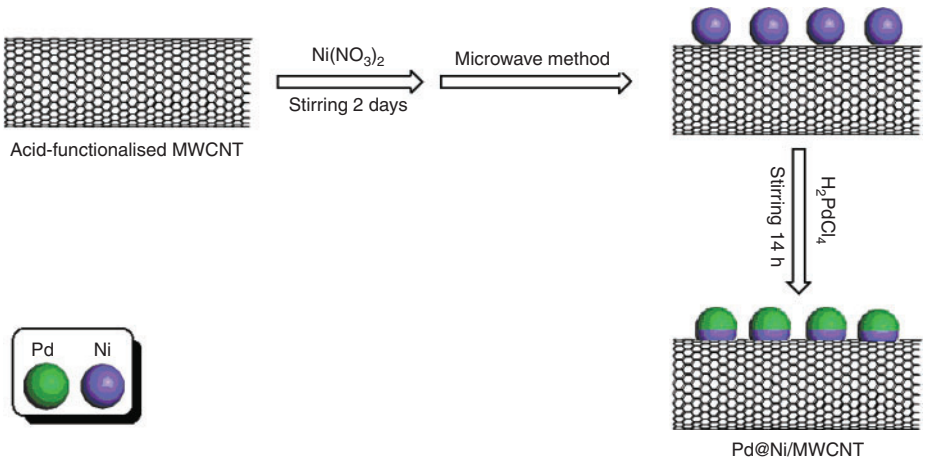

Fig. 1. Schematic diagram of the synthesis of Pd@Ni nanocatalysts on multiwalled carbon nanotubes (MWCNT).

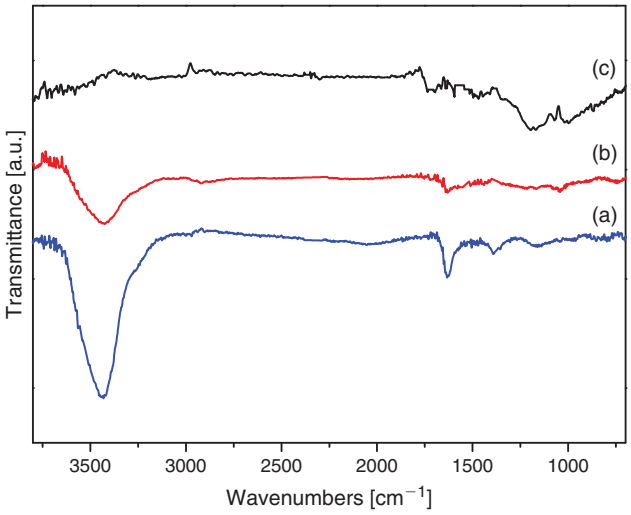

Fig. 2. FTIR spectra of H_2SO_4/HNO_3-treated multiwalled carbon nanotubes (a) (MWCNT), (b) HNO_3-treated MWCNT, and (c) untreated MWCNT.

we can see that the dispersion of Pd@Ni nanoparticles on acid-treated MWCNT is very uniform. Moreover, Ni nanoparticles supported on acid-treated MWCNT with a diameter ranging from 6 to 10 nm can be observed (Fig. 3c), evidencing that EG successfully made the Ni impregnated in MWCNT transform into monocrystalline nickel nanoparticles at 180°C under microwave heating in a microwave oven. The elemental analysis by EDS proved that the Ni/MWCNT are composed of C and Ni. TEM was further used to explore the morphology of Pd@Ni nanoparticles on MWCNT composites (Fig. 3d). It shows a large number of extremely small nanoparticles distributed homogeneously on the external surface of the acid-treated MWCNT. Furthermore, the Pd@Ni nanoparticles on the MWCNT have a narrow size range from 3 to 6 nm with regular shapes. The high-resolution TEM image describing the crystalline nature of the Pd@Ni nanoparticles is shown in Fig. 3f. The single crystalline Pd@Ni particles have lattice planes with an interlayer distance of 0.203 nm, which are indexed to Ni (111) crystal planes. The outer layer of the nanoparticles show a different contrast, with the parallel lattice fringes measured as 0.224 nm, which corresponds to Pd (111) planes. It can be inferred that the Ni particles were supported on the MWCNT first, and then the Pd particles coated the Ni nanoparticles. At the same time Pd particles were fixed to the MWCNT because the bottom of the Pd also contacted with the MWCNT. Possibly, both palladium and nickel nanoparticles have strong interactions with the MWCNT surface, which restrains the aggregation and the growth of the nanoparticles to form larger particles, resulting in the uniform distribution of these nanoparticles. The particle size distribution derived from the TEM results (the insets in Fig. 4a, b) further illustrate this. The elemental analysis by EDS (Fig. 4a) proved that the Ni/MWCNT are composed of C and Ni. It is seen that Pd@Ni nanoparticles supported on pristine MWCNT (Fig. 5a) show an uneven distribution and aggregation in comparison with Pd@Ni nanoparticles supported on acid-treated MWCNT (Fig. 5b). Thus, it can provide us with straightforward information that acid-treated MWCNT contain abundant oxygen functional groups on the surface, which can efficiently disperse metal nanoparticles and result in a higher catalytic activity.

XRD Analysis

The crystal structure and the phase purity of MWCNT, Ni/MWCNT, Pd/MWCNT, and Pd@Ni/MWCNT particles were determined by XRD as shown in Fig. 6a. The broad peaks at $2\theta = 26.07°$ are associated with C (002) planes of the graphite-like structure of the MWCNT. The other five peaks of the Pd@Ni/MWCNT are characteristic of face centred cubic (fcc) crystalline Pd and Ni, corresponding to the planes of Ni (111), (200), and (220) at 2θ values of ~44.81°, 51.99°, and 76.62°, and Pd (111), (200), and (220) at 2θ values of ~40.26°, 46.81°, and 68.27°. Fig. 6a reveals an obvious shift in the position of the Ni (200) peak in the Pd@Ni/MWCNT compared with that in the Ni/MWCNT (Fig. 6a, curve b). The shift of the diffraction peak reveals that there is strong interaction between partial Ni and Pd.[32,33] The peaks of Pd are obviously stronger than the diffraction peak of Ni in Fig. 6a, curve d, which further suggests that Ni atoms form a core with Pd atoms partly forming an outside layer. As displayed in Fig. 6b, a positive shift of the Pd peaks occur for Pd@Ni/MWCNT compared with the Pd/MWCNT, indicating that the Ni atoms enter into the Pd crystals which causes the narrow transformation of the Pd crystal lattice distance. During the aerobic selective oxidation of an alcohol it has been demonstrated that the Pd (111) plane is the

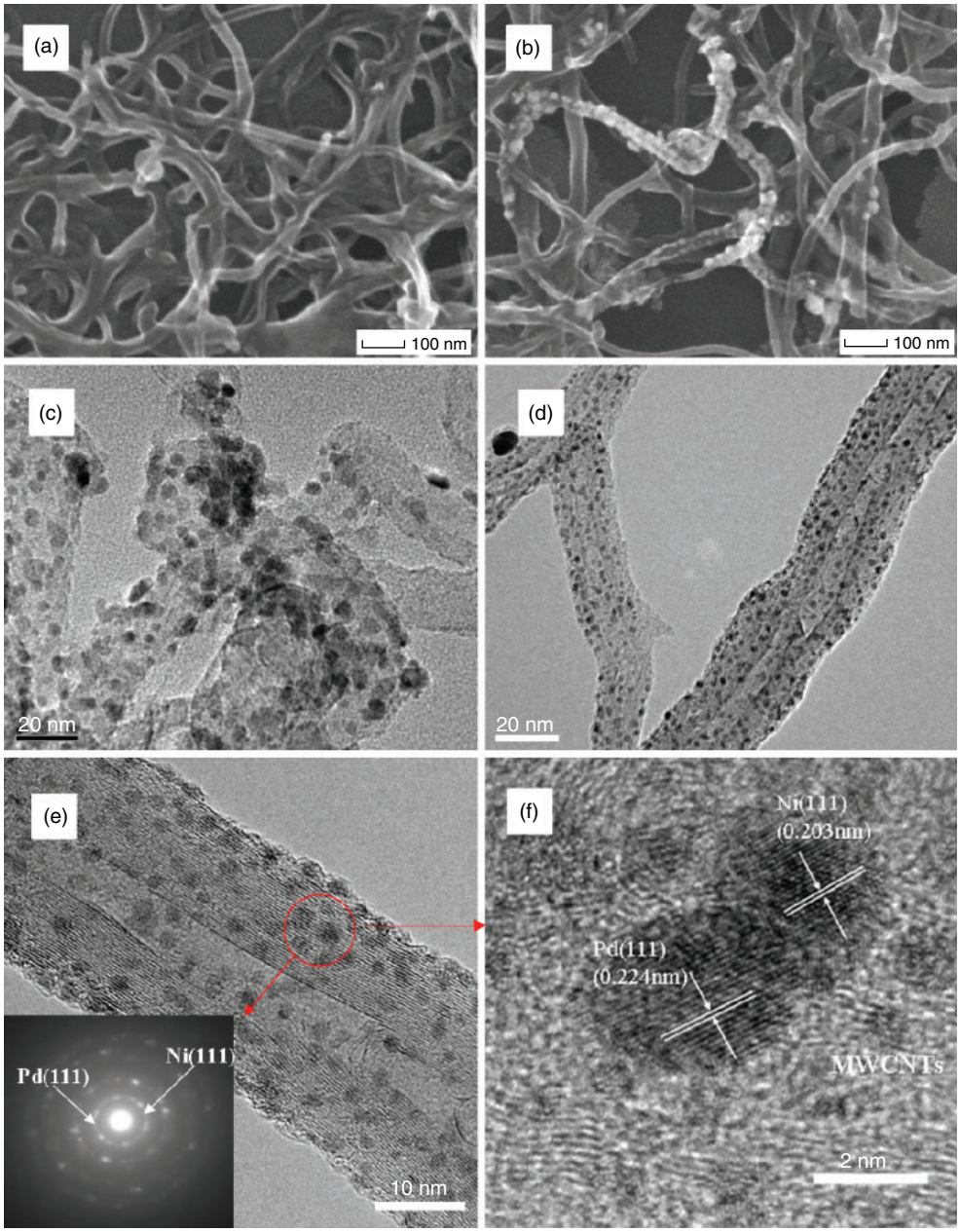

Fig. 3. Field effect scanning electron microscopy images of (a) acid-treated multiwalled carbon nanotubes (MWCNT) and (b) Pd@Ni/MWCNT. Transmission electron microscopy (TEM) images of (c) Ni/MWCNT and (d) Pd@Ni/MWCNT. Magnified TEM image of Pd@Ni/MWCNT (the inset is the corresponding SAED pattern) (e). (f) High-resolution TEM image of Pd@Ni/MWCNT.

catalytic centre and most alcohols and O_2 are adsorbed and desorbed on it.[34] The relatively strong diffraction peak of the Pd (111) plane in Fig. 6a, curve d, reveals that the as-made catalyst has catalytically active centres and can promote the selective oxidation of alcohols. Based on the Scherer's equation shown below (Eqn 1) and the full width half-maximum peak of the Pd (111) crystal plane, the average crystalline sizes of all these samples were estimated according to the line width analysis of the Pd (111) diffraction peak. As can be seen, the crystal mean size is found to be 4.0 nm for Pd@Ni/MWCNT

$$D = \frac{0.89\lambda}{\beta \cdot \cos\theta} \quad (1)$$

where D is the average particle size, $\lambda = 0.15406$ nm (XRD wavelength corresponding to $Cu_{K\alpha}$ radiation), β is the width (radians) of the peak at half height, and θ is the diffraction angle.

Pd@Ni/MWCNT as Catalysts for Selective Oxidation of Benzyl Alcohol

The catalytic activity of Pd@Ni/MWCNT nanoparticles for the oxidation of benzyl alcohol is systematically examined. Clean catalytic syntheses in water under mild conditions are highly desirable processes from an economic to environmental point of view. Therefore, water as the reaction media and hydrogen peroxide (H_2O_2) as oxygen resources are chosen. Considering their high activity and low cost, Pd@Ni nanoparticles are

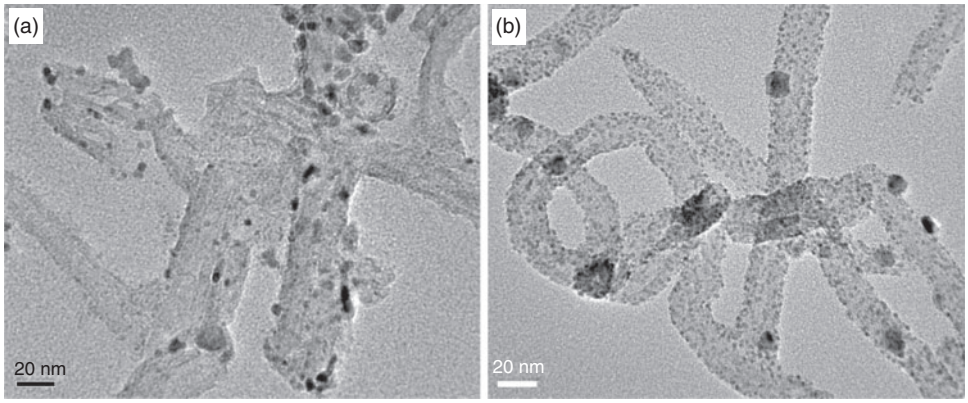

Fig. 4. Energy-dispersive X-ray spectroscopy spectra of (a) Ni/multiwalled carbon nanotube (MWCNT) and (b) Pd@Ni/MWCNT composites The insets in (a) and (b) are the size distribution of the metal particles on Ni/MWCNT and Pd@Ni/MWCNT derived from TEM images, which were established from the measurements of 100 particles.

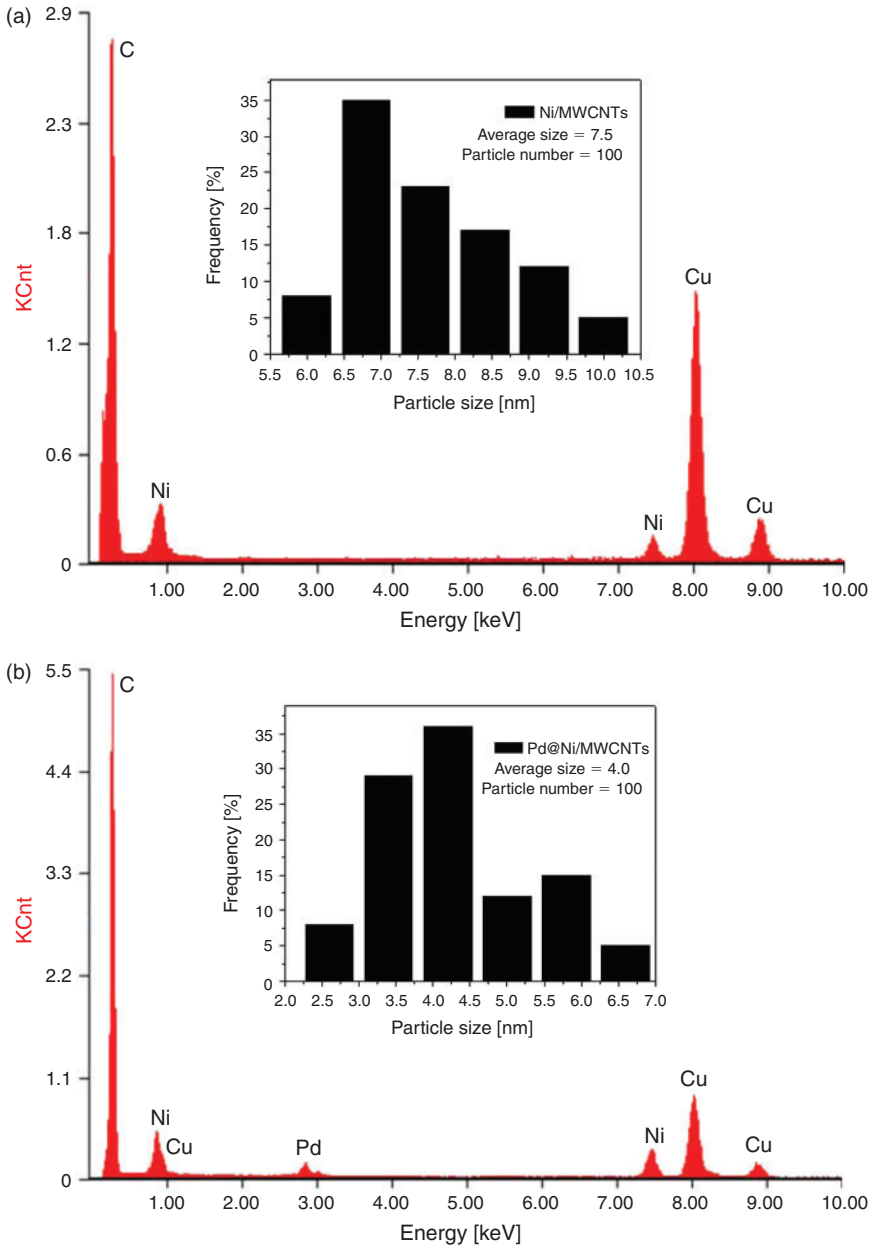

Fig. 5. Transmission electron microscopy images of (a) Pd@Ni nanoparticles on pristine multiwalled carbon nanotubes (MWCNT) and (b) Pd@Ni nanoparticles on acid-treated MWCNT.

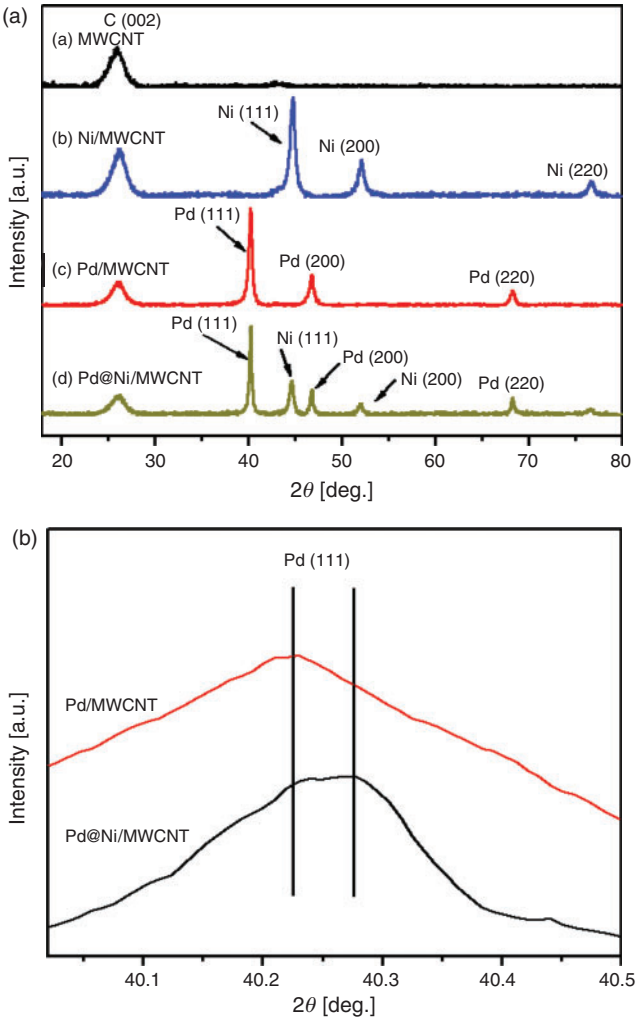

Fig. 6. Typical X-ray diffraction pattern of (a) multiwalled carbon nanotubes (MWCNT), (b) Ni/MWCNT, (c) Pd/MWCNT, and (d) Pd@Ni/MWCNT.

Table 1. Benzyl alcohol oxidation catalyzed by Pd@Ni/multiwalled carbon nanotube nanoparticles with different amounts of catalyst

Benzyl alcohol (3 mmol), K_2CO_3 (6 mmol), water, H_2O_2, 6 h

Entry	Catalyst [mmol]	Benzyl alcohol conversion [%]	Selectivity [%]		
			Benzaldehyde	Benzoic acid	Benzyl benzoate
1	0.05	31	56	38	6
2	0.10	54	70	26	4
3	0.15	72	91	7	6
4	0.18	89	91	7	2
5	0.2	99	98	4	2
6	0.22	90	88	9	3

initially selected as catalysts for the oxidation of benzyl alcohol. First, we examine the effect of catalyst amount on the alcohol conversion and aldehyde selectivity. The products are mainly aldehyde and acid, while an ester is also found in some cases. As shown in Table 1, a low amount of catalyst results in low alcohol conversion, and the products are mostly a mixture of aldehyde and acid. By increasing the catalyst amount from Pd 0.05 to 0.2 mmol, the alcohol conversion increased and so did the

Table 2. Benzyl alcohol oxidation catalyzed by Pd@Ni/multiwalled carbon nanotubes at different times

Benzyl alcohol (2 mmol), K_2CO_3 (6 mmol), catalyst (Pd: 0.2 mmol), H_2O_2, water, 80°C

Entry	Time [h]	Benzyl alcohol conversion [%]	Selectivity [%]		
			Benzaldehyde	Benzoic acid	Benzyl benzoate
1	1	40	51	45	4
2	2	59	64	33	3
3	4	73	85	12	3
4	5	82	90	5	5
5	6	99	98	2	1
6	7	94	88	7	5

Table 3. Benzyl alcohol oxidation catalyzed by Pd@Ni/multiwalled carbon nanotubes at different temperatures

Benzyl alcohol (2 mmol), K_2CO_3 (6 mmol), catalyst (Pd: 0.2 mmol), water, H_2O_2, 6 h

Entry	Temperature [°C]	Benzyl alcohol conversion [%]	Selectivity [%]		
			Benzaldehyde	Benzoic acid	Benzyl benzoate
1	30	75	54	44	2
2	40	79	62	35	3
3	60	81	75	21	4
4	80	99	98	1	2
5	90	94	90	7	3

selectivity of the aldehyde. However, a further increase of catalyst amount led to a decrease of both alcohol conversion and aldehyde selectivity. With 0.2 mmol of Pd catalyst, high alcohol conversion (99 %) and aldehyde selectivity (98 %) can be achieved.

The reaction times are also investigated, which is shown in Table 2. The conversion of benzyl alcohol increased with time and then became steady; however, the selectivity of the aldehyde showed a maximum at a time of 6 h. This implies that increasing the reaction time will not contribute to alcohol conversion and is not beneficial for selectivity of an aldehyde product.

The influence of reaction temperature on the benzyl alcohol conversion and benzaldehyde selectivity is also studied. As listed in Table 3, the alcohol conversion and aldehyde selectivity increase with temperature, especially the alcoholconversion, which could reach as high as 99 % at 80°C. However, it should be noted that if the temperature continued to increase, the selectivity for benzaldehyde will decrease. So we choose 80°C as the reaction temperature.

The catalytic performance of the different catalysts for the oxidation of benzyl alcohol are presented in Table 4. The catalytic activity of Ni/MWCNT was very poor. Although a high selectivity with the Pd-rich catalyst (Pd/MWCNT) was observed, the conversion was obviously lower than for Pd@Ni/MWCNT catalysts at the same Pd loadings. The enhanced catalytic activity has been attributed to several factors, including the interaction between the metal and the MWCNT,[35] d-band centre shift,[24] and crystal nickel entering into the palladium crystal lattice leading to a synergistic effect. Zhao et al. used density functional theory (DFT) calculations to show that extra

Table 4. Benzyl alcohol oxidation catalyzed by different metal-deposited multiwalled carbon nanotube (MWCNT) catalysts at the same conditions

Benzyl alcohol (2 mmol), K_2CO_3 (6 mmol), catalyst (0.2 mmol), water, H_2O_2, 80°C, 6 h

Catalyst	Benzyl alcohol conversion [%]	Selectivity [%]		
		Benzaldehyde	Benzoic acid	Benzyl benzoate
Ni/MWCNT	10	6	2	2
Pd/MWCNT	91	94	3	3
Pd@Ni/MWCNT 3	99	98	1	1

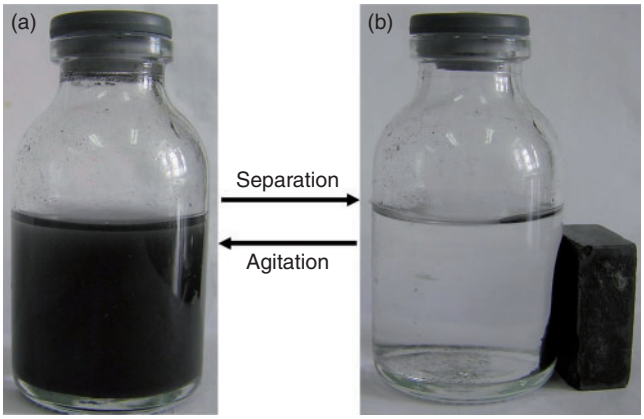

Fig. 7. The states of Pd@Ni/multiwalled carbon nanotube particles: (a) without a magnetic field and (b) in a magnetic field.

Ni–C bonds form at the interface, as such, more electrons transfer from the interfacial C–C bonds to the Ni–C bonds.[35] The interaction between Ni atoms and Pd atoms, such as the space change of the Pd crystal lattice induced by the filling of Ni atoms, impart Pd@Ni/MWCNT with a fairly conductive network to allow facile charge-transfer and mass-transfer processes. Studies have found that the space change of a noble metal crystal lattice could improve catalytic activity.[24]

After oxidation, the reaction solution was transferred into a vessel and a magnet was placed on the outside of the vessel wall. It is observed that the magnetic Pd@Ni/MWCNT particles can be separated from aqueous solution under an external magnetic field, and can be redispersed into the water with agitation, as shown in Fig. 7. In the absence of an external magnetic field, the dispersion of the Pd@Ni/MWCNT particles was visibly dark and homogeneous (Fig. 7a). When the external magnetic field was applied, the Pd@Ni/MWCNT particles aggregated, leading to transparency of the dispersion (Fig. 7b). This phenomenon reveals that the Pd and MWCNT do not affect the magnetic properties of the Ni nanoparticles during the synthesis process. The Pd@Ni/MWCNT catalyst quickly adsorbed onto the wall of the vessel and the catalyst was then collected and washed with ethanol and deionised water three times and dried at 60°C, for reuse. The recycling performance of the catalyst is shown in Table 5. The catalyst exhibited a high catalytic activity with high conversion and selectivity. In addition, the change in structure and composition of the Ni after several catalytic cycles of benzyl alcohol oxidation, determined by XRD patterns, were compared. From the XRD pattern we can clearly see that the

Table 5. Recycling of the Pd@Ni/multiwalled carbon nanotube catalyst for the oxidation of benzyl alcohol

Benzyl alcohol (3 mmol), K_2CO_3 (6 mmol), catalyst (Pd: 0.2 mmol), water, H_2O_2, 80°C, 6 h

Cycle number	Conversion [%]	Selectivity [%]
1	99	98
2	92	95
3	87	96
4	84	92

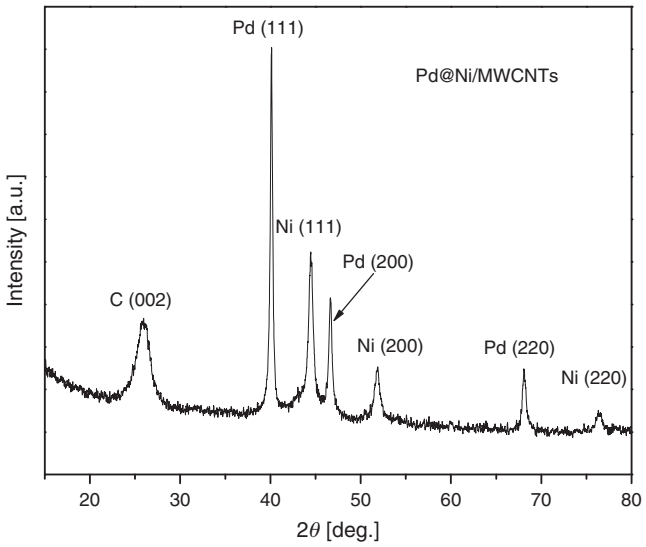

Fig. 8. Typical X-ray diffraction pattern of Pd@Ni/multiwalled carbon nanotubes (MWCNT) after four catalytic cycles.

characteristic peaks of the catalyst do not show obvious changes both before and after reaction. Other characteristic peaks such as for NiO were not visualised by the XRD pattern, as shown in Fig. 8. With subsequent reuse the selectivity remains almost the same. Nevertheless, the conversion decreased the catalytic activity gradually over time. This phenomenon might be attributed to the partial aggregation of Pd@Ni nanoparticles after several recycles. In summary, Pd@Ni/MWCNT have relatively good stability and give good recycle performance.

Conclusions

A magnetically recoverable Pd@Ni bimetallic nanoparticle catalyst supported on MWCNT was successfully prepared by a simple method. The as made catalyst gave high catalytic activity towards the selective oxidation of benzyl alcohol under relatively mild conditions in the presence of H_2O_2. A green highly effective route was thus achieved for the transformation of benzyl alcohol to benzaldehyde and the selective synthesis of other aromatic or aliphatic aldehydes is also expected. The results indicated that benzaldehyde could be obtained in a high yield and selectivity from benzyl alcohol using the Pd@Ni/MWCNT catalyst in water as a solvent in the presence of H_2O_2 as an oxygen source at 80°C in 6 h. The catalyst can be easily separated magnetically and a high catalytic activity was retained after recycling the catalyst four times in comparison with the pure MWCNT carriers and the Pd noble metal catalysts. It is implied that Pd nanoparticles supported on Ni/MWCNT are

very promising for portable applications in the selective oxidation of benzyl alcohol to aldehyde and is valuable for the development of other MWCNT-based metallic catalyst systems.

Acknowledgements

This work was supported financially by the Jiangsu Science and Technology Support Program (BE2010144), Zhenjiang industry supporting plan (GY2010020), and the Research Foundation for Talented Scholars of Jiangsu University (11JDG149). Dr M. M. Zhang acknowledges the support of the Innovation Funds of Jiangsu University (CXLX12_0647).

References

[1] D. I. Enache, J. K. Edwards, P. Landon, B. Solsona-Espriu, A. F. Carley, A. A. Herzing, M. Watanabe, C. J. Kiely, D. W. Knight, G. J. Hutchings, *Science* **2006**, *311*, 362. doi:10.1126/SCIENCE.1120560

[2] J. Han, Y. Liu, L. Li, R. Guo, *Langmuir* **2009**, *25*, 11054. doi:10.1021/LA901373T

[3] L. Wang, L. Shen, X. Xu, L. Xu, Y. Qian, *RSC Advances, 2* **2012**, 10689. doi:10.1039/C2RA21325G

[4] G. F. Zhao, H. Y. Hu, M. M. Deng, Y. Lu, *Chem. Commun.* **2011**, *47*, 9642. doi:10.1039/C1CC12964C

[5] X. C. Chen, Y. Q. Hou, H. Wang, Y. Cao, J. H. He, *J. Phys. Chem. C* **2008**, *112*, 8172. doi:10.1021/JP800610Q

[6] A. Villa, D. Wang, N. Dimitratos, D. S. Su, V. Trevisan, L. Prati, *Catal. Today* **2010**, *150*, 8. doi:10.1016/J.CATTOD.2009.06.009

[7] Z. X. Yan, M. Cai, P. K. Shen, *J. Mater. Chem.* **2012**, *22*, 2133. doi:10.1039/C1JM14765J

[8] Z. X. Yan, C. X. Wang, P. K. Shen, *Int. J. Hydrogen Energy* **2012**, *37*, 4728. doi:10.1016/J.IJHYDENE.2011.04.113

[9] Y. Z. Xiang, Y. A. Lv, T. Y. Xu, X. N. Li, J. G. Wang, *J. Mol. Catal. Chem.* **2011**, *351*, 70. doi:10.1016/J.MOLCATA.2011.09.018

[10] K. Deplanche, I. P. Mikheenko, J. A. Bennett, M. Merroun, H. Mounzer, J. Wood, L. E. Macaskie, *Top. Catal.* **2011**, *54*, 1110. doi:10.1007/S11244-011-9691-0

[11] C. Della Pina, E. Falletta, M. Rossi, *J. Catal.* **2008**, *260*, 384. doi:10.1016/J.JCAT.2008.10.003

[12] S. Marx, A. Baiker, *J. Phys. Chem. C* **2009**, *113*, 6191. doi:10.1021/JP808362M

[13] D. Matthey, J. G. Wang, S. Wendt, J. Matthiesen, R. Schaub, E. Laegsgaard, B. Hammer, F. Besenbacher, *Science* **2007**, *315*, 1692. doi:10.1126/SCIENCE.1135752

[14] K. C. Mondal, L. M. Cele, M. J. Witcomb, N. J. Coville, *Catal. Commun.* **2008**, *9*, 494. doi:10.1016/J.CATCOM.2007.07.043

[15] S. H. Sun, G. X. Zhang, D. S. Geng, Y. G. Chen, M. N. Banis, R. Y. Li, M. Cai, X. L. Sun, *Chem. – Eur. J.* **2010**, *16*, 829.

[16] Z. Liu, E. T. Ada, M. Shamsuzzoha, G. B. Thompson, D. E. Nikles, *Chem. Mater.* **2006**, *18*, 4946. doi:10.1021/CM060973J

[17] H. Y. Zhang, Y. Xie, Z. Y. Sun, R. T. Tao, C. L. Huang, Y. F. Zhao, Z. M. Liu, *Langmuir* **2011**, *27*, 1152. doi:10.1021/LA1034728

[18] P. Panagiotopoulou, D. I. Kondarides, *Catal. Today* **2006**, *112*, 49. doi:10.1016/J.CATTOD.2005.11.026

[19] Y. C. Zhao, X. L. Yang, J. N. Tian, F. Y. Wang, L. Zhan, *Int. J. Hydrogen Energy* **2010**, *35*, 3249. doi:10.1016/J.IJHYDENE.2010.01.112

[20] M. Shao, K. Sasaki, N. S. Marinkovic, L. Zhang, R. R. Adzic, *Electrochem. Commun.* **2007**, *9*, 2848. doi:10.1016/J.ELECOM.2007.10.009

[21] D. Chen, J. Li, C. Shi, X. Du, N. Zhao, J. Sheng, S. Liu, *Chem. Mater.* **2007**, *19*, 3399. doi:10.1021/CM070182X

[22] R. Harpeness, A. Gedanken, *Langmuir* **2004**, *20*, 3431. doi:10.1021/LA035978Z

[23] S. Nath, S. Praharaj, S. Panigrahi, S. K. Ghosh, S. Kundu, S. Basu, T. Pal, *Langmuir* **2005**, *21*, 10405. doi:10.1021/LA051710R

[24] R. R. Adzic, J. Zhang, K. Sasaki, M. B. Vukmirovic, M. Shao, J. X. Wang, A. U. Nilekar, M. Mavrikakis, J. A. Valerio, F. Uribe, *Top. Catal.* **2007**, *46*, 249. doi:10.1007/S11244-007-9003-X

[25] Z. J. Wang, Q. X. Zhang, D. Kuehner, X. Y. Xu, A. Ivaska, L. Niu, *Carbon* **2008**, *46*, 1687. doi:10.1016/J.CARBON.2008.07.020

[26] S. Y. Wang, S. P. Jiang, T. J. White, J. Guo, X. Wang, *J. Phys. Chem. C* **2009**, *113*, 18935. doi:10.1021/JP906923Z

[27] K. Sasaki, R. R. Adzic, *J. Electrochem. Soc.* **2008**, *155*, B180. doi:10.1149/1.2816238

[28] B. H. Wu, Y. J. Kuang, X. H. Zhang, J. H. Chen, *Nano Today* **2011**, *6*, 75. doi:10.1016/J.NANTOD.2010.12.008

[29] H. B. Chu, L. Wei, R. L. Cui, J. Y. Wang, Y. Li, *Coord. Chem. Rev.* **2010**, *254*, 1117. doi:10.1016/J.CCR.2010.02.009

[30] J. P. Cheng, X. B. Zhang, F. Liu, J. P. Tu, Y. Ye, Y. J. Ji, C. P. Chen, *Carbon.* **2003**, *41*, 1965. doi:10.1016/S0008-6223(03)00185-4

[31] H. Xu, L. P. Zeng, S. J. Xing, G. Y. Shi, Y. Z. Xian, L. T. Jin, *Electrochem. Commun.* **2008**, *10*, 1839. doi:10.1016/J.ELECOM.2008.09.030

[32] A. Tegou, S. Papadimitriou, I. Mintsouli, S. Armyanov, E. Valovab, G. Kokkinidis, S. Sotiropoulos, *Catal. Today* **2011**, *170*, 126. doi:10.1016/J.CATTOD.2011.01.003

[33] M. C. Zhao, C. Rice, R. I. Masel, P. Waszczuk, A. Wieckowskib, *J. Electrochem. Soc.* **2004**, *151*, A131. doi:10.1149/1.1630806

[34] A. F. Lee, Z. Chang, P. Ellis, S. F. J. Hackett, K. Wilson, *J. Phys. Chem. C* **2007**, *111*, 18844. doi:10.1021/JP709944C

[35] M. T. Zhao, W. Xiao, H. J. Zhang, K. Cho, *Phys. Chem. Chem. Phys.* **2011**, *13*, 11657. doi:10.1039/C0CP02910F